Supplemental Material for "Making Aircraft Vortices Visible to Radar by Spraying Water into the Wake"*

Karim Shariff
NASA Ames, Moffett Field, California, 94035

August 16, 2016

*Journal of Atmospheric & Oceanic Technology, 2016

Contents

This document contains Supplemental Material for a 2016 article in the Journal of Atmospheric and Oceanic Technology.

The two sub-sections below use the abbreviation PK for the book by Pruppacher and Klett (1997). The subscripts 'a' and 'w' denote air and water, respectively. Symbols that have already been defined in the main text are not redefined here.

A Drag coefficient

With the Reynolds number defined as $\mathrm{Re} \equiv 2a|\mathbf{u}_{\mathrm{rel}}|/\nu_{\mathrm{a}}$ (where ν_{a} is the kinematic viscosity of air), the coefficient of drag, C_{D}, is obtained by numerically inverting the relation (PK, Equation 10-145):

$$Y = \sum_{m=0}^{6} B_m X^m, \tag{1}$$

where $X = \ln(C_{\mathrm{D}}\mathrm{Re}^2)$ and $\mathrm{Re} = \exp(Y)$. This formula is originally from Beard (1976) and is based on the drag coefficient of a solid sphere. The validity of this rests on two assumptions. The first is that the droplet does not distort significantly from being spherical. The equilibrium aspect ratio of a falling raindrop is given by PK (Equation 10-108):

$$\frac{b}{a} = \frac{1 - 0.11\mathrm{We}}{1 + 0.11\mathrm{We}}. \tag{2}$$

Here $\mathrm{We} \equiv 2a\rho_{\mathrm{a}}u_{\mathrm{rel}}^2/\gamma_{\mathrm{w/a}}$ is the Weber number, where $\gamma_{\mathrm{w/a}}$ is the surface tension of water in air. For nozzle 1 and the IFR case, the smallest value of b/a was 0.9 which occurred at early times for a droplet which quickly fell below the vortex. We conclude that droplet deformation is negligible particularly for those droplets that remain with the vortex pair. The second assumption is that the ratio of

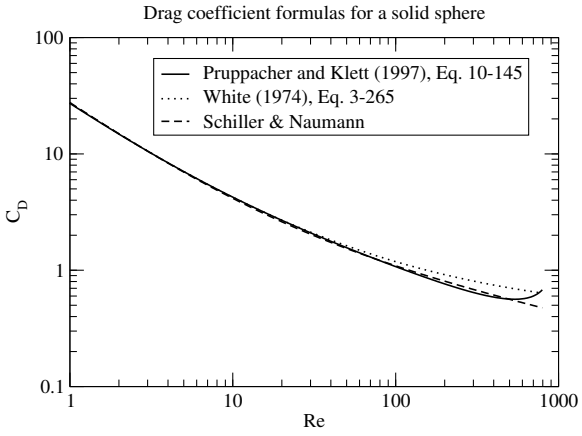

Figure 1: Comparison of three formulas for the drag coefficient of a solid sphere.

dynamic viscosities, $\eta_{\rm a}/\eta_{\rm w} \approx 1.8 \times 10^{-2}$ is small. In the creeping flow limit, the Hadamard-Rybczynski formula (see Beard 1976) for the drag of a water sphere divided by the drag of a solid sphere is

$$\frac{F_{\rm D}}{F_{{\rm D}s}} = 1 - \eta_{\rm a}/3\eta_{\rm w} = 0.995. \tag{3}$$

Numerical solutions (PK, p. 388) indicate that for Re < 300, the drag coefficient of a water sphere differs by less than $\sim 1\%$ from that of a solid sphere.

Formula (1) is valid for Re < 500. Only for nozzle 4 was this condition slightly exceeded for a few droplets. For Re ≤ 1.5, the explicit formula for solid spheres (White, 1974, eq. 3-265) was found to agree well with (1) and was used instead. We have also implemented but not used the Schiller and Naumann explicit drag formula for a solid sphere (e.g., Apte et al., 2003)

$$C_{\rm D} = \frac{24}{\rm Re}\left((1 + 0.15{\rm Re}^{0.687}\right) \tag{4}$$

which is said to be accurate to within 5% for Re < 800. Figure 1 compares the three formulas for $C_{\rm D}$ up to the maximum value of Re $= 800$ we allow in the code. It suggests that in the future it would be as accurate to use the explicit Schiller and Naumann formula, which is cheaper to compute.

B Evaporation model

The evaporation model uses appropriate formulas from PK. These formulas are collected here to document the choices we have made and also because they are scattered throughout the book. Gas kinetic effects and the Kelvin curvature effect are neglected since we remove droplets when their radii fall below 20 μm.

Throughout, $T_{\rm C}$ denotes centigrade temperature:

$$T_{\rm C} = T - 273.15. \tag{5}$$

Note that there are 100 Pa in a mb. Subscripts 'a' and 'w' denote air and water, respectively.

B.1 Properties of air, liquid water, and water vapor

Given the universal gas constant, $\mathcal{R} = 8.3144$ J K^{-1} mol^{-1}, and the molar mass of dry air, $M_{\rm a} = 28.9644 \times 10^{-3}$ kg mol^{-1}, the gas constant for air is

$$R_{\rm a} = \mathcal{R}/M_{\rm a}. \tag{6}$$

The density of air is calculated from the ideal gas law:

$$\rho_{\rm a} = p/R_{\rm a}T. \tag{7}$$

The density of liquid water at $p = 1$ atm is given by (PK 3-13):

$$10^3\rho_{\rm w} = \frac{\sum_{m=0}^{5} A_m {T_{\rm C}}^m}{1 + BT} \text{ g cm}^{-3},\ 0 \le T_{\rm C} \le 100, \tag{8}$$

with $A_0 = 999.8396, A_1 = 18.224944, A_2 = -7.922210\times10^{-3}, A_3 = -55.44846\times 10^{-6}, A_4 = 149.7562 \times 10^{-9}, A_5 = -393.2952 \times 10^{-12}, B = 18.159725 \times 10^{-3}$. The thermal diffusivity of air is

$$\kappa_{\rm a} = k_{\rm a}/\rho_{\rm a}C_p, \tag{9}$$

where the conductivity is given by (PK 13-18a):

$$k_{\rm a} = (5.69 + 0.017T_{\rm C}) \times 10^{-5} \text{ cal cm}^{-1} \text{ s}^{-1} \text{ K}^{-1}. \tag{10}$$

Note that there are 4.184 J per cal. The heat capacity of air is:

$$C_p = 1006.1 \text{ J kg}^{-1} \text{ K}^{-1}. \tag{11}$$

The diffusivity, $D_{\rm v}$, of water vapor is calculated using Equation (PK 13-3):

$$D_{\rm v} = 0.211 \left(\frac{T}{T_0}\right)^{1.94} \left(\frac{p_0}{p}\right) \text{cm}^2 \text{ s}^{-1}, \tag{12}$$

with $T_0 = 273.15$ K and $p_0 = 1013.25$ mb. The dynamic viscosity of air is (PK 10-141)

$$\eta_{\rm a} = (1.718 + 0.0049T_{\rm C}) \times 10^{-4} \text{ poise},\ T_{\rm C} \ge 0. \tag{13}$$

The Schmidt number of vapor is defined (PK , p. 538) as

$$\text{Sc}_{\rm v} \equiv \nu_{\rm a}/D_{\rm v}, \tag{14}$$

where $\nu_{\rm a} = \eta_{\rm a}.\rho_{\rm a}$ is the kinematic viscosity. The Schmidt number for heat is

$$\text{Sc}_{\rm h} \equiv \nu_{\rm a}/\kappa_{\rm a}. \tag{15}$$

B.2 Evolution of droplet radius

The evolution of droplet radius $a(t)$ is given by:

$$a\frac{da}{dt} = \left(a\frac{da}{dt}\right)_0 f_\mathrm{v}, \tag{16}$$

where f_v, called the ventilation coefficient, represents the enhancement of evaporation rate due to advection of air past the droplet, and $()_0$ represents a quantity in the absence of advection.

Let $\mathrm{Re} = 2aU_\mathrm{rel}/\nu_\mathrm{a}$ denote the Reynolds number based on droplet diameter and drop speed U_rel relative to the air. Defining $F \equiv \mathrm{Sc}_\mathrm{v}^{1/3}\mathrm{Re}^{1/2}$, the ventilation coefficient is given by (PK 13-60) and (PK 13-61):

$$f_\mathrm{v} = \begin{cases} 1.00 + 0.108F^2, & F < 1.4; \\ 0.78 + 0.308F, & 1.4 \le F < 51.4. \end{cases} \tag{17}$$

The first factor on the RHS of (16), which represents evaporation in the absence of advection, is given by

$$\left(a\frac{da}{dt}\right)_0 = \frac{D_\mathrm{v}M_\mathrm{w}}{\mathcal{R}\rho_\mathrm{w}}\left(\frac{e_\infty}{T_\infty} - \frac{e_\mathrm{sat}(T_a)}{T_a}\right), \tag{18}$$

where D_v is the vapor diffusivity (which we evaluated at ambient conditions using equation 12), $M_\mathrm{w} = 28.97$ gm mol^{-1} is the molecular mass of water, e_∞ is the vapor pressure in the ambient, T_∞ is the ambient temperature, and $e_\mathrm{sat}(T_a)$ is the saturation vapor pressure evaluated at the surface temperature T_a of the droplet. For $e_\mathrm{sat}(T)$ we use the expression (Sonntag, 1994, eq. 7)

$$e_\mathrm{sat}(T) = 100\exp\left(\sum_{m=1}^{4} a_m T^{m-2} + a_5 \ln T\right) \text{ Pa}, \ 173.15 \le T \le 373.15, \tag{19}$$

with $a_1 = -6.0969385 \times 10^3, a_2 = 1.6635794 \times 10^1, a_3 = -2.711193 \times 10^{-2}, a_4 = 1.673952 \times 10^{-5}, a_5 = 2.433502$.

B.3 Temperature at the droplet surface

The internal energy of the water droplet is:

$$q = mC_\mathrm{w}T_a, \tag{20}$$

where m is its mass, $C_\mathrm{w} = 4.187 \times 10^3$ J kg^{-1} K^{-1} is the heat capacity of water, and T_a is its temperature, which we have taken to be uniform and equal to the value at the surface. The internal energy of the drop increases due to diffusion of heat at its surface and release of latent heat (PK 13-65):

$$\frac{dq}{dt} = 4\pi f_\mathrm{h} a k_\mathrm{a}(T_\infty - T_a) + L_\mathrm{e}\frac{dm}{dt}, \tag{21}$$

where L_e is the latent enthalpy of evaporation of pure water evaluated at the surface temperature of the drop. The dependence of L_e on centigrade temperature T_C is:

$$L_\mathrm{e} = \left(2500.8 - 2.36T_\mathrm{C} + 0.0016{T_\mathrm{C}}^2 - 0.00006{T_\mathrm{C}}^3\right) \times 10^3 \text{ J kg}^{-1}. \quad (22)$$

Substituting (20) into (21) gives

$$\frac{dT_a}{dt} = \frac{3f_\mathrm{h}k_{\mathrm{a}\infty}}{C_\mathrm{w}a^2\rho_\mathrm{w}}\left(T_\infty - T_a\right) + 3(L_\mathrm{e}/C_\mathrm{w} - T_a)\frac{1}{a}\frac{da}{dt}. \quad (23)$$

Here f_h is the ventilation coefficient for heat: it is given by the same expression as (17) except with $F = \mathrm{Sc_h}^{1/3}\mathrm{Re}^{1/2}$, where $\mathrm{Sc_h}$ is the Schmidt number for heat.

C Upper bound for the rate of coagulation

Here we briefly address the issue of droplet coagulation, which was raised by the second referee. First, recall that for a given volume, droplet coagulation improves radar reflectivity until the radius of droplets becomes larger than about 200 μm, at which point they begin to descend faster than the wake. Let n_1 and n_2 denote the number density of droplets in radius bins $[a_1, a_1 + da_1]$ and $[a_2, a_2 + da_2]$, respectively. The rate $\dot{n}_{12}$ (per unit volume) at which droplets in the two groups combine is expressed as

$$\dot{n}_{12} = n_1 n_2 K(a_1, a_2), \quad (24)$$

where $K(a_1, a_2)$ is called the coagulation kernel. Although the subject is still evolving, there has been progress in developing models for $K(a_1, a_2)$ in turbulent flow; we employ the one given in Riemer and Wexler (2005). It requires two parameters to characterize the turbulence, namely, the rate of dissipation (ϵ_t) of turbulent kinetic energy per unit mass, and the rms of velocity fluctuations (u_rms). Data presented by Ahmad and Proctor (2012) for five days in August 1995 at Memphis International Airport show that in the absence of thunderstorms, diurnal peak values were $\epsilon_\mathrm{t} \approx 2 \times 10^{-3}$ m^2 s^{-3} and $u_\mathrm{rms} \approx 1.4$ m s^{-1} (their Figures 13 and 14). We produced a plot of $K(r_1, r_2)$ for this case and it indicated a maximum value of $K_\mathrm{max} = 7.9 \times 10^{-6}$ m^3 s^{-1}. The rate of all coagulation events (per unit volume) is

$$\begin{aligned}\dot{n}_\mathrm{coagulations} = \sum_{ij,j\geq i} n_i n_j K(a_i, a_j) &\approx \frac{1}{2}\sum_{ij} n_i n_j K(a_i, a_j) \\ &\leq \frac{1}{2}K_\mathrm{max}\sum_{ij} n_i n_j = \frac{1}{2}K_\mathrm{max}n^2, \quad (25)\end{aligned}$$

where

$$n \equiv \sum_i n_i, \quad (26)$$

is the total number density. The approximation sign becomes an equality in the continuous limit. We therefore obtain the upper bound

$$\dot{n}_{\text{coagulations}} \leq \frac{1}{2} K_{\max} n^2. \tag{27}$$

The peak value of n in our simulation (for the IFR case) is ≈ 250 m^{-3}. Therefore $\dot{n}_{\text{coagulations}} \leq 0.25$ m^{-3} s^{-1}, which implies ≤ 36 coagulation events per m^3 during the 144 s of wake evolution time corresponding to a distance of 6 nm behind the aircraft. During convective activity in the atmosphere, the data of Ahmad and Proctor (2012) give $\epsilon_{\text{t}} = 1000$ cm^2 s^{-3} and $u_{\text{rms}} = 4.2$ m s^{-1} for which we find that $K_{\max} = 6.5 \times 10^{-6}$ m^3 s^{-1}. This value is surprisingly less than for the previous case considered (the reason for which is not understood). We conclude that in future studies, coagulation should be included. However, on the basis of the above estimates, we do not expect its effect on radar reflectivity to be catastrophic in most situations.

D dBZ values

Designers of rain and cloud radars usually want to know the value of dBZ they should design a radar system to detect. Here

$$Z(\mathbf{x}) \equiv \sum_{i}^{N} D_i^6 / \text{Vol}(\mathbf{x}), \tag{28}$$

where Vol($\mathbf{x}$) is the volume of a region centered at $\mathbf{x}$, D_i is the diameter of the ith droplet in the volume, and N is the number of droplets in the volume. To be meaningful, $Z(\mathbf{x})$ must be independent of Vol($\mathbf{x}$) for the range of radar resolution volumes considered. This might be true for a large patch of rain or cloud. However, it is not true in the present case: both the outer size of the droplet spiral and its inner length scale (the characteristic distance between spiral turns) is in the range of typical radar resolution volumes. With this caveat, Figure 2 presents plots of dBZ for the IFR (high humidity) and non-IFR (average humidity) cases considered in the paper. Here Z has units of mm^6 m^{-3} and Vol($\mathbf{x}$) was taken to be the cylindrical resolution volume centered at $\mathbf{x}$ with length equal to $c\tau/2$ and radius equal to $R(\mathbf{x})\theta_{\text{b}}$, with $\tau = 0.2$ μs and $\theta_{\text{b}} = 0.52°$. The range $R(\mathbf{x})$ is measured from the radar location whose coordinates are $(x_{\text{rad}}, y_{\text{rad}}, z_{\text{rad}}) = (6 \text{ nm}, -0.67 \text{ nm}, -582 \text{ m})$ relative to the aircraft.

E Can airborne radar detect a spray trail?

Figure 3a shows SNR1 for a Collins WXR-2100 airborne radar located at $x = 6$ nm behind the generating aircraft and at $z = 0$ (the altitude at which the vortex was generated). The radar parameters are: $f = 9.33$ GHz, peak power,

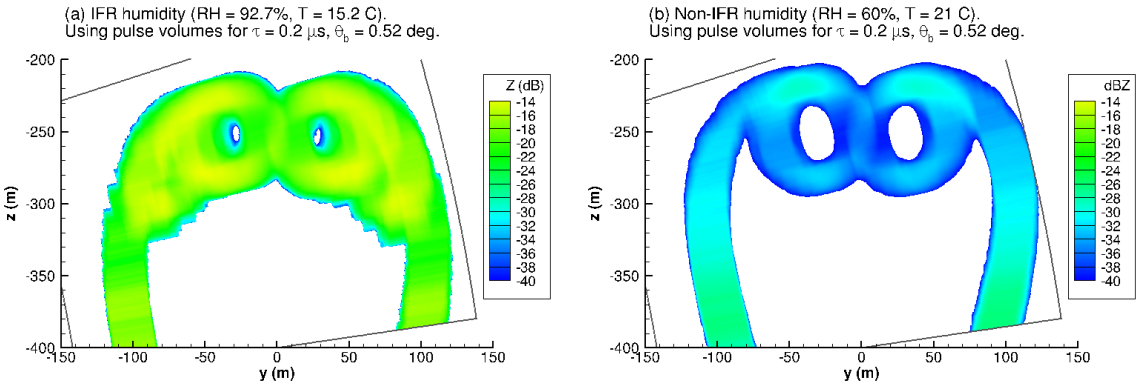

Figure 2: dB$Z(\mathbf{x})$ with Z in mm^6 m^{-3} using cylindrical volumes of length $c\tau/2$ and radius $R(\mathbf{x})\theta_\mathrm{b}$ with $\tau = 0.2$ μs and $\theta_\mathrm{b} = 0.52°$. (a) IFR humidity (RH = 92.7%, T = 15.2 C). (b) Non-IFR humidity (RH = 60%, T = 21 C). Nozzle 1.

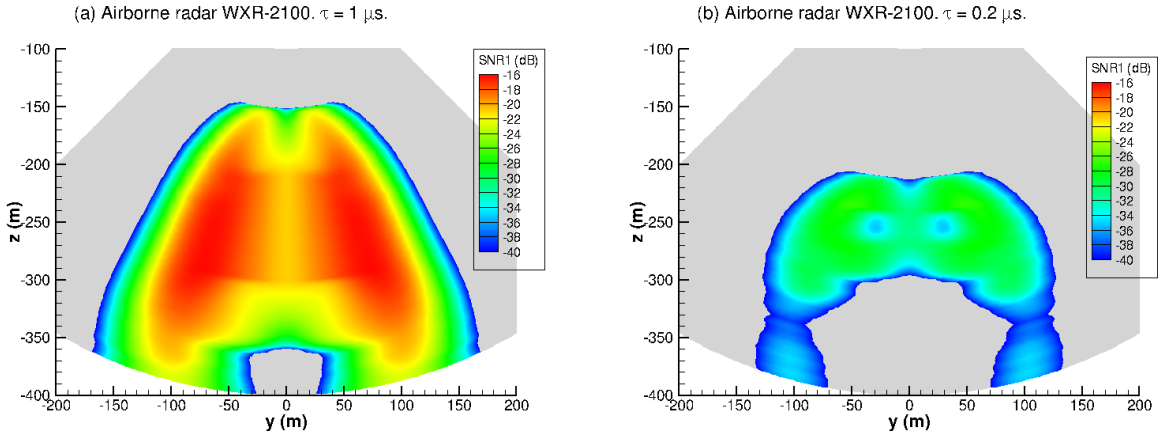

Figure 3: Simulated SNR1 for the Collins WXR-2100 airborne weather radar located above the wake at $x = 6$ nm behind the aircraft and pointed downward. Pulse widths: (a) $\tau = 1$ μs; (b) $\tau = 0.2$ μs. IFR humidity: RH = 92.7%, $T = 15.2$ C. Nozzle 1.

P_t = 150 W; beamwidth, $\theta_b = 10°$; receiver noise figure, NF = 3.8 dB. The shortest available pulse width of $\tau = 1$ μs was chosen. Waveguide and finite bandwidth loss factors were chosen to be the same as that for the radars listed in Table 4 of the paper. For simplicity, the antenna is pointed straight downward, whereas in reality it would be tilted downward at a smaller angle relative to the fuselage; this would result in a larger range and less SNR1. Figure 3a shows that to detect the spray trail, both resolution and sensitivity needs to be improved from their current values, the latter by at least 26 dB. Figure 3b shows that resolution is improved if a $\tau = 0.1$ μs pulse is provided, however, this would require the sensitivity to be improved even more. Another issue to keep in mind is the highly non-steady nature of the target arising from motion of the airplane.

References

N. Ahmad, Nash'at and F.H. Proctor. Estimation of eddy dissipation rates from mesoscale model simulations. Paper 2012-0429, AIAA, 2012.

S. Apte, M. Gorokhovski, and P. Moin. LES of atomizing spray with stochastic modeling of secondary breakup. *Intl. J. Multiphase Flow*, 29:1503–1522, 2003. doi: 10.1016/S0301-9322(03)00111-3.

K.V. Beard. Terminal velocity and shape of cloud and precipitation drops aloft. *J. Atmos. Sci.*, 33:851–864, May 1976. doi: 10.1175/1520-0469(1976)033%3C0851:TVASOC%3E2.0.CO;2.

H.R Pruppacher and J.D. Klett. *Microphysics of clouds and precipitation.* Kluwer, Dordrecht, 1997.

N. Riemer and A.S. Wexler. Droplets to drops by turbulent coagulation. *J. Atmos. Sci.*, 62:1962–1975, June 2005. doi: dx.doi.org/10.1175/JAS3431.1.

D. Sonntag. Advancements in the field of hygrometry. *Meteorol. Zeitschrift*, 3: 51–66, 1994.

F.M. White. *Viscous Fluid Flow.* McGraw-Hill, New York, 1974.